Water Dissociation on Clean and Boron-Modified Single-Crystal $Ni_3(Al,Ti)$ (110) Surfaces†

Jinliu Wang and Yip-Wah Chung*

Department of Materials Science and Engineering, Robert R. McCormick School of Engineering and Applied Science, Northwestern University, Evanston, Illinois 60208

Received: September 21, 1999; In Final Form: January 10, 2000

The interaction of water vapor with clean and boron-modified $Ni_3(Al,Ti)$ surfaces was studied with temperature-programmed desorption, X-ray photoemission, and Auger electron spectroscopy. Thermal desorption results indicate that water dissociates on clean boron-free $Ni_3(Al,Ti)$ (110) surfaces, resulting in hydrogen evolution at ~400 K. X-ray photoemission studies show that water dissociation occurs above 190 K. Hydrogen desorption at ~400 K is completely suppressed by boron adsorption at a coverage of about 0.3 monolayer. Auger and X-ray photoemission studies on boron-modified $Ni_3(Al,Ti)$ (110) surfaces show that boron reacts with water to form hydroxyl at 130−190 K. Hydrogen desorption occurs at ~950 K from boron-modified $Ni_3(Al,Ti)$ (110) surfaces, indicating strong B−H bonding.

Introduction

Ni_3Al with the face-centered-cubic $L1_2$ structure[1] is attractive for structural applications at high temperatures.[2] This is mainly because of the anomalous temperature dependence of the flow stress of Ni_3Al, which increases with temperature, reaching a peak value at about 800 °C.[3] In addition, Ni_3Al has low density due to the presence of aluminum and tends to form an adherent aluminum oxide layer at high temperature, which protects the base material from excessive oxidation and corrosion. However, Ni_3Al has a major disadvantage—polycrystalline Ni_3Al has low tensile ductility and suffers brittle fracture at room temperature.[4]

George et al.[5] demonstrated that the ductility of Ni_3Al at room temperature is a strong function of the test environment. Experimental results have shown that moisture-induced embrittlement is the major cause of the low ductility and intergranular failure of Ni_3Al and other intermetallic alloys.[6] It was proposed that water reacts with fresh reactive surfaces (cracks) formed during tensile deformation to produce atomic hydrogen. The atomic hydrogen then penetrates into crack tips and causes hydrogen embrittlement. By carefully studying the water dissociation reaction on different $Ni_3(Al,Ti)$ single-crystal surfaces, Chia and Chung[7,8] revealed that water dissociation on the $Ni_3(Al,Ti)$ surface is structure-sensitive. The $Ni_3(Al,Ti)$ (111) surface is inactive toward water dissociation, while the (100) surface is active. These findings imply that the ductility of polycrystalline intermetallics is dependent on the orientation of grain boundaries relative to the stress axis because cracks usually initiate from grain boundaries during mechanical testing.

It was first reported in 1979 that the ductility of Ni_3Al is dramatically improved by microalloying with boron, which occupies interstitial sites.[9] A tensile ductility as high as 50% at room temperature has been achieved in Ni_3Al-based alloys by doping with only 0.1 wt % boron.[10] Beryllium was also found to improve the ductility of Ni_3Al, although to a lesser degree.[11] However, carbon, which is also an interstitial in Ni_3Al, does not induce any beneficial effect.[12,13]

Many investigations were carried out in the past decade to explore the beneficial effect of boron on the ductility improvement of Ni_3Al. Liu et al.[10,14,15] found that boron exhibits a strong tendency to segregate to grain boundaries of Ni_3Al, although the extent of segregation appears to vary from boundary to boundary. On the basis of this observation, they proposed that boron segregation may serve two functions: increasing the cohesion of grain boundaries and suppressing the environmental effect. They also noticed that boron segregation appears to vary with the aluminum concentration—boron segregation decreases by 45% as the aluminum concentration increases from 24 to 25.2 at. %.[10] However, the work of Briant and Taub[16] did not show clear dependence of boron segregation on the aluminum concentration of Ni_3Al.

Another model[17−19] to explain the boron effect is based on the localized composition disorder induced by boron segregation to grain boundaries. This may facilitate slip transfer across grain boundaries, thereby resulting in less stress concentration and reduced crack nucleation at grain boundaries. King and Yoo[20] showed theoretically that slip transmission across the grain boundary is indeed easier if it is disordered.

The mechanism by which boron suppresses the embrittlement of Ni_3Al has not been directly explored before this work. One previous investigation introduced boron to the specimen surface by dissociating diborane (B_2H_6) in an ion gun.[21] Though this may be a valid approach, the excess hydrogen may have played some unpredictable role.

To elucidate the role of boron in affecting the surface reactions of water vapor and hydrogen with single-crystal Ni_3Al surfaces, we adopted a different approach to introduce controlled surface coverage of boron. Using a cesium-based solid electrolyte, we can extract cesium ions (Cs^+) to bombard a boron target. The cesium ions serve two functions: (i) they eject boron by sputtering; (ii) deposition of cesium reduces the work function of the surface so that B^- emission becomes favorable. This process provides a clean source of low-energy boron ions whose energy and flux can be adjusted for our surface dosing experiments. In this article, we explored the interaction between water vapor and boron-modified $Ni_3(Al,Ti)$ (110) using thermal desorption, X-ray photoemission and Auger electron spectroscopy.

† Part of the special issue "Gabor Somorjai Festschrift".

* Corresponding author. Phone: (847)-491-3112. E-mail: ywchung@nwu.edu.

10.1021/jp993388x CCC: $19.00
Published on Web 02/11/2000

Experiment

All experiments were carried out in a bakeable stainless steel ultrahigh vacuum chamber with a base pressure of 5×10^{-10} Torr equipped with sputtering, gas handling, Auger electron spectroscopy, X-ray photoemission spectroscopy (XPS), residual gas analysis (RGA), and low-energy negative boron ion source capabilities. Photoelectron spectra were collected with a double-pass cylindrical mirror analyzer set at a pass energy of 50 eV using the Al $K\alpha_{1,2}$ radiation at 1486.6 eV. Surface cleaning was done with several cycles of Ar-ion bombardment at 2 kV, 45° angle of incidence, followed by annealing at ~1000 K for 30 min. A Skion negative ion beam source (Model: NMIBS-CS02) was used to dose the sample with boron ions at 50−150 eV. The surface coverage of boron (θ_B) was determined separately by Auger calibration. One boron monolayer is defined as 1.1×10^{15} atoms/cm^2 (cf. the (110) plane atom density is 1.1×10^{15} atoms /cm^2).

In this study, D_2O was used to minimize unwanted H_2O and H_2 contributions from the background. The gas was purified by multiple freeze−pump−thaw cycles. D_2O was admitted into the chamber through a needle doser placed ~1 cm from the sample. All gas exposures were expressed in Langmuir units where 1 Langmuir (L) = 1×10^{-6} Torr s. To achieve different gas exposures, a constant uncorrected pressure of 1×10^{-7} Torr was maintained for different lengths of time. Deuterium and hydrogen are taken as equivalent in the following discussion.

The sample can be heated to ~1000 K using a tungsten wire radiation heater mounted behind the sample or cooled to ~90 K via a copper contact with a liquid-nitrogen reservoir. Temperatures were measured by a K-type (chromel−alumel) thermocouple spot-welded to the sample. Temperature-programmed desorption (TPD) experiments were performed at a heating rate of 2−2.5 K/s. A glass envelope was mounted in front of the RGA ionizer. During thermal desorption, the sample was placed in front of this envelope to minimize detection of background desorption. Generally, due to the cracking of D_2O in the RGA ionizer, a small D_2 signal accompanies D_2O desorption. This contribution (~3% of the D_2O signal) was subtracted in all thermal desorption data.

Single crystals of Ni_3(Al,Ti) with 75 at. % Ni, 20 at. % Al, 5 at. % Ti were used in this study. Five atomic percent of Ti was added to Ni_3Al to facilitate single-crystal growth. The Bridgman technique was used to grow Ni_3(Al,Ti) single crystals. Details of crystal growth were described elsewhere.[7,8] From the ternary phase diagram[22,23] and X-ray diffraction results,[24] Ti was found to substitute Al atoms in Ni_3Al. Addition of 5 at. % Ti does not appear to affect the environmental sensitivity of Ni_3Al.[25,26] After obtaining the required orientation using the back-reflection Laue method, single-crystal samples were wire-cut to about 10 mm diameter and 2 mm thickness. Each wafer was mechanically polished using standard metallographic techniques, with the final step using 0.05 μm Al_2O_3, and then electropolished in a solution of 90% methanol, 10% sulfuric acid at 12 V, 273 K. We used the (110) orientation for the present study.

Results and Discussion

Water Adsorption on Clean Ni_3(Al,Ti) (110). Figure 1 is a typical Auger spectrum of a clean Ni_3(Al,Ti) (110) surface after a few cycles of argon ion sputtering and annealing at 1000 K under ultrahigh vacuum. The sample was then cooled to 90 K and exposed to 20 L of D_2O (all filaments off during exposure). Temperature-programmed desorption from the Ni_3(Al,Ti) (110) surface followed with the RGA monitoring signal at $m/e = 4$ (D_2) and 20 (D_2O). Figure 2 shows desorption peaks of D_2O around 160 and 190 K. According to previous studies on water adsorption on Ni (111) surface by Stulen and Thiel,[27] the desorption peak at 160 K was interpreted as due to the sublimation of ice layers, while the peak at 190 K was attributed to the desorption of the first adsorbed water layer. As shown in Figure 2, D_2 evolution also occurred, peaking at ~400 K. The desorption of D_2 after exposure of D_2O to the Ni_3(Al,Ti) (110) surface indicates that some water molecules dissociate into atomic hydrogen. This is similar to our previous work on clean Ni_3(Al,Ti) (100), which gives a D_2 thermal desorption peak at ~330 K under otherwise identical conditions.[8]

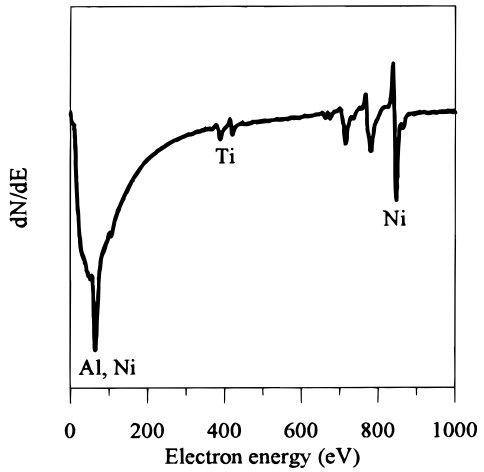

Figure 1. Auger electron spectrum from the clean Ni_3(Al,Ti) (110) surface.

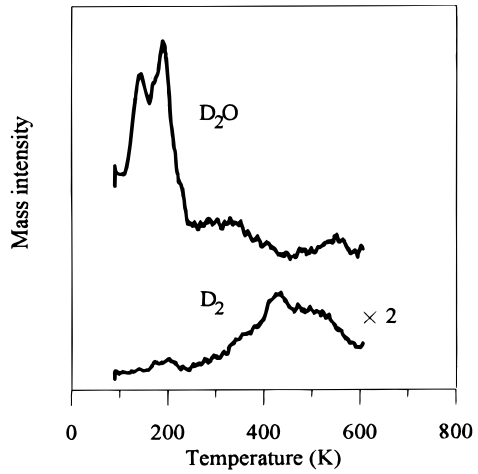

Figure 2. Thermal desorption of D_2O ($m/e = 20$) and D_2 ($m/e = 4$) from the Ni_3(Al,Ti) (110) clean surface after 20 layer D_2O exposure at 90 K.

X-ray photoemission studies were carried out to explore the chemical state of oxygen. Figure 3 shows the oxygen 1s core level spectra after water adsorption on the (110) surface at 130 K, followed by slow warming. At 145−192 K, the oxygen 1s binding energy is 534.2−534.5 eV, which is close to the reported data for adsorbed water.[28−32] Therefore, we interpret this to be due to water/ice adsorbed as intact molecules. With increasing temperature, the oxygen 1s peak decreases in intensity (due to D_2O desorption) and shifts to smaller binding energy. At 192−272 K, the oxygen 1s peak is at 532.2−532.8 eV, which is due to adsorbed OD.[33,34] The presence of hydroxyl indicates the partial dissociation of water. This dissociation appears to start at ~190 K. At 278−388 K, the major O 1s peak is still at 532.1 eV, while a small shoulder appears at ~530.8 eV. At 388−473

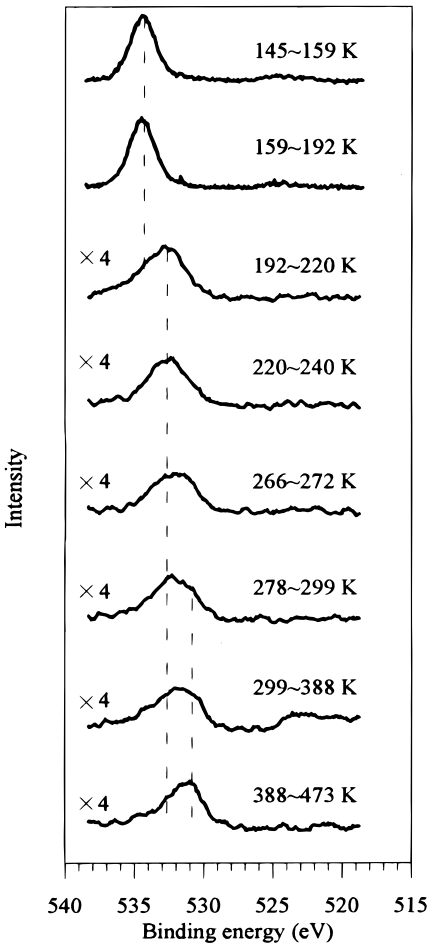

Figure 3. X-ray photoemission spectra of O 1s taken at different temperatures after 3 layer D_2O exposure to the clean boron-free Ni_3(Al,Ti) (110) surface at 130 K.

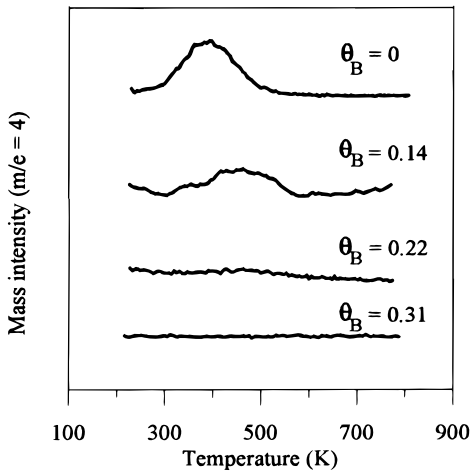

Figure 4. Thermal desorption of D_2 ($m/e = 4$) from the Ni_3(Al,Ti) (110) surface after 10 layer D_2O exposure at 110 K with different boron coverages.

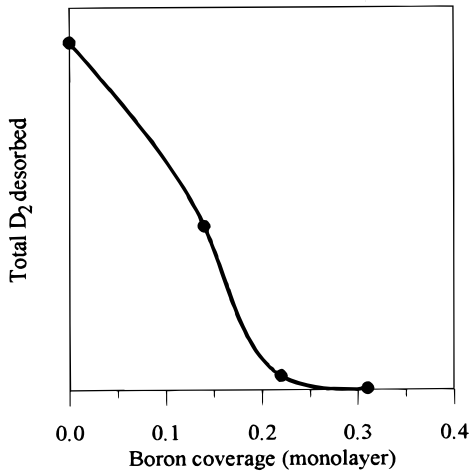

Figure 5. Variation of total D_2 desorbed from the Ni_3(Al,Ti) (110) surface (as measured from the area under the desorption peak at ~400 K) versus boron coverage.

K, the oxygen 1s peak binding energy shifts to 530.8 eV, which is due to atomic oxygen.[35] This chemical shift is attributed to the complete dissociation of water. These XPS studies indicate that water dissociation to produce atomic hydrogen occurs on clean boron-free Ni_3(Al,Ti) (110) above ~190 K.

Water Adsorption on Boron-Modified Ni_3(Al,Ti) (110). Immediately after sputter-cleaning and annealing at ~1000 K, we allowed the single-crystal sample to cool. Boron dosing began at a sample temperature <700 K. Above 700 K, we observed little or no boron Auger signal, either due to low sticking probability or (more likely) dissolution into the bulk crystal. After boron dosing and further cooling to 110 K, the Ni_3(Al,Ti) sample was exposed to 10 L of D_2O, followed by thermal desorption. The desorption of D_2O from the boron-modified Ni_3(Al,Ti) (110) surface is essentially the same as the clean surface, i.e., two desorption peaks at 160 and 190 K. The desorption of D_2, however, is significantly modified. Figure 4 shows thermal desorption spectra of D_2 at a boron coverage θ_B of 0, 0.14, 0.22, and 0.31. Figure 5 plots the total amount of desorbed D_2 versus boron coverage, showing the strong suppression of D_2 production around 400 K by surface boron.

Auger electron spectroscopy was used to follow the chemical state of boron before and after D_2O exposure (Figure 6). The boron peak is at 179 eV before D_2O exposure (curve a). After D_2O dosing at 100 K, the intensity slightly decreases (probably due to attenuation), and the peak is still at 179 eV (curve b). When the sample was heated to 190−198 K (curve c), there is a small shoulder at 170 eV, which increases in intensity with further temperature increase to 215 K (curve d). The peak at 170 eV is believed to be due to oxidized boron. Kiss and Solymosi[36] studied water adsorption on boron-contaminated Rh (111) and Rh foil surfaces. They found that upon water dissociation, the boron Auger peak shifts from 179−182 to 168−172 eV, which was believed to result from the formation of B−O species.

Figure 7 shows the O 1s core level spectra on the boron-modified Ni_3(Al,Ti) (110) surface after water exposure. At about 130 K, there are obviously two peaks, one at 535.6 eV due to water and one at 532.9 eV due to hydroxyl. With increasing temperature, the O 1s peak binding energy shifts to 532.7 eV, characteristic of adsorbed hydroxyl. There is no observable change of peak shape and intensity up to about 280 K. A small shoulder emerges at ~530 eV above 282 K. This is due to adsorbed atomic oxygen. At 350−456 K, the O 1s peak slightly broadens and can be deconvoluted into two peaks, one at 532.7 eV due to hydroxyl and the other at 529.7 eV due to atomic oxygen. The above photoemission studies were done for the surfaces with different boron coverages from 0.10 to 0.91 monolayer. The results show a trend similar to that in Figure 7.

The formation of hydroxyl at ~130 K indicates that boron-modified Ni_3(Al,Ti) (110) dissociates water at a lower temperature than the clean boron-free (110) surface. Combined with above Auger studies, we believe that water dissociation in the

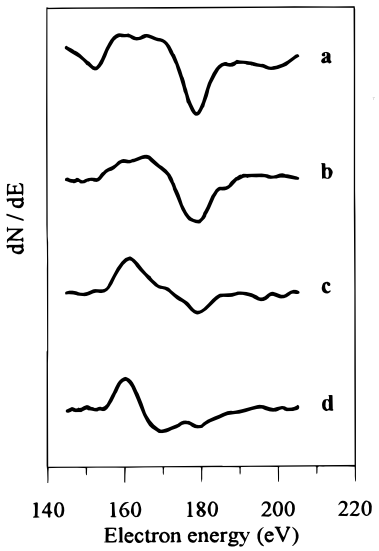

Figure 6. Auger electron spectrum of boron taken (a) after 0.16 monolayer boron dosing to the $Ni_3(Al,Ti)$ (110) surface. After 1 layer D_2O exposure at 100 K, the spectra were taken at (b) 100 K, (c) 190−198 K, and (d) 215 K.

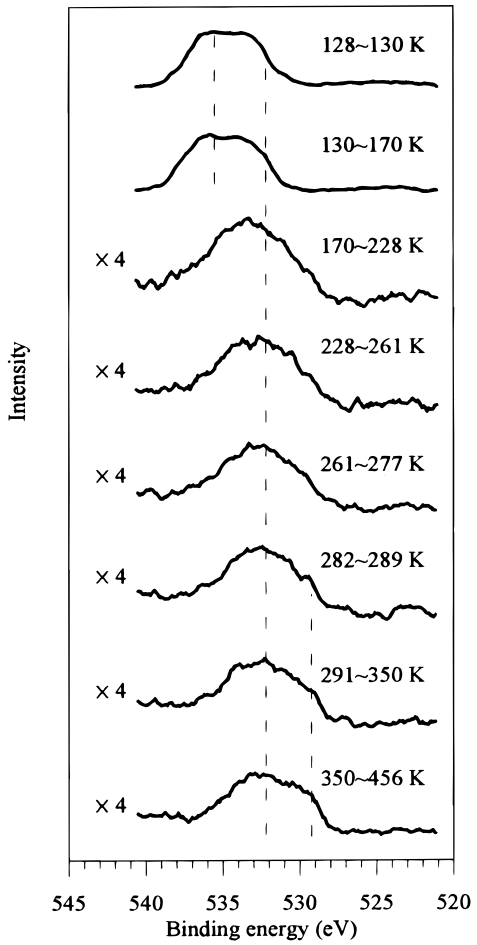

Figure 7. X-ray photoemission spectra of O 1s taken at different temperatures after 4 layer D_2O exposure to a 0.10 monolayer boron-modified $Ni_3(Al,Ti)$ (110) surface at 130 K.

presence of boron occurs between 130 and 190 K. This dissociation might be due to the high stability of the B−O bond. The B−O bond dissociation energy is 809 kJ/mol.[37] The surface reaction of boron with water on the Ta (110) surface to form B−O bond has been reported before.[38]

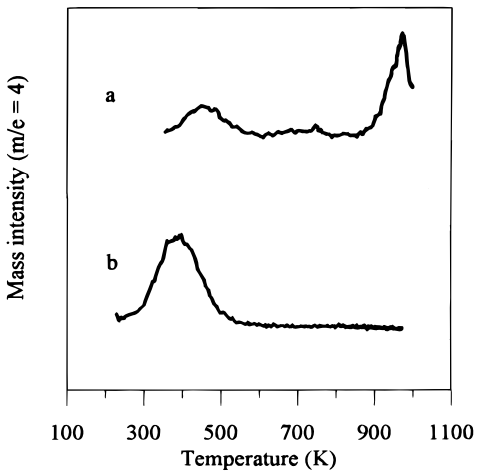

Figure 8. Thermal desorption of D_2 ($m/e = 4$) (a) from 0.15 monolayer boron-modified $Ni_3(Al,Ti)$ (110) after 10 layer D_2O exposure at 130 K and (b) from boron-free $Ni_3(Al,Ti)$ (110) exposed to 10 layers of D_2O at 130 K.

Now the question is: why is there no hydrogen evolution around 400 K? To investigate this, we used temperature-programmed desorption with maximum temperature up to about 1000 K. After dosing the surface with 0.15 monolayer of boron followed by 10 layers of D_2O at 130 K, we performed temperature-programmed desorption. The heating rate at 130−750 K was about 2 K/s, while the heating rate above 750 K was 0.5−1.5 K/s. Figure 8 curve a shows a new D_2 desorption peak from the boron-modified surface at ∼950 K. This unusually high desorption temperature may be explained by the formation of a strong B−D bond (bond dissociation energy is 341 kJ/mol[37]). Furthermore, since boron dissolves into the bulk crystal at >700 K, it is possible that deuterium is "pulled" into the bulk at the same time. To remove dissolved boron, we back-filled the chamber with 1×10^{-7} Torr oxygen (99.9999% purity) with the $Ni_3(Al,Ti)$ crystal heated to about 623 K for 20 min. Auger electron spectroscopy showed that boron is drawn to the surface by oxygen. The surface was then sputter-cleaned and annealed at ∼1000 K. This procedure was repeated until no boron Auger signal was detectable. Figure 8 curve b shows the thermal desorption of D_2 from this clean surface after 10 layer D_2O exposure at 130 K. We observed only one major D_2 desorption peak at ∼400 K, as shown earlier, and there is no D_2 thermal desorption at higher temperature. This provides strong evidence that the D_2 desorption peak at ∼950 K from the boron-modified surface is due to boron.

D_2 desorption at ∼950 K on the boron-modified $Ni_3(Al,Ti)$ (110) surface indicates that atomic hydrogen is strongly adsorbed to the surface up to and above 700 K. According to our previous study,[7,8] aluminum is the active species in controlling water dissociation on clean boron-free $Ni_3(Al,Ti)$ surfaces. Atomic hydrogen resulting from water dissociation sits mainly on Ni sites. On boron-modified $Ni_3(Al,Ti)$ surfaces, B−O species produced by water dissociation are believed to be very stable (B−O bond dissociation energy is 809 kJ/mol) and act as inert spectators on the surface. Atomic hydrogen is the embrittlement species so that the key issue is where it sits on boron-modified surfaces. Since the B−H bond dissociation energy (340 kJ/mol) is significantly greater than that for Ni−H (252 kJ/mol),[37] atomic hydrogen might prefer to sit on boron sites. In this case, atomic hydrogen on boron-modified $Ni_3(Al,Ti)$ surfaces is likely to be less mobile than on boron-free surfaces at room temperature. During room-temperature tensile testing of boron-doped Ni_3Al in moist air, this should result in a lower concentration of atomic

hydrogen at the crack tip, thus suppressing hydrogen-induced embrittlement.

Conclusions

The interaction between water vapor and a single-crystal $Ni_3(Al,Ti)$ (110) surface with and without boron was investigated by temperature-programmed desorption and Auger and X-ray photoemission studies. Hydrogen-free boron dosing was provided by a solid-state boron ion source. Water dissociates into atomic hydrogen on the clean $Ni_3(Al,Ti)$ (110) surface above 190 K, and the resulting hydrogen desorbs at ~400 K. The hydrogen desorption peak at ~400 K is completely suppressed by boron adsorption at coverage ≥ 0.3 monolayer. Boron reacts with water and is partially oxidized at 130−190 K. The resulting hydrogen desorption at ~950 K from the boron-modified $Ni_3(Al,Ti)$ surface indicates that boron is strongly bonded to atomic hydrogen (produced by water dissociation). This strong B−H bonding suppresses the desorption, and most likely the diffusion of atomic hydrogen to the crack tip. These results provide a natural explanation to the suppression of moisture-induced embrittlement of Ni_3Al and related alloys by boron.

Acknowledgment. This work is supported by the National Science Foundation, grant no. DMR 9713052.

References and Notes

(1) Van Deen, J. K.; Van Der Woude, F.; Drijver, J. W. *Scripta Metall.* **1978**, *12*, 161.
(2) Milligan, W. W.; Antolovich, S. D. *Metall. Trans. A* **1989**, *20*, 2811.
(3) Stoloff, N. S. *Int. Mater. Rev.* **1989**, *34*, 153.
(4) Copley, S. M.; Kear, B. H. *Trans. TMS-AIME* **1967**, *239*, 977.
(5) George, E. P.; Liu, C. T.; Pope, D. P. *Scripta Metall. Mater.* **1994**, *30*, 37.
(6) Liu, C. T. *Scripta Metall. Mater.* **1992**, *27*, 25.
(7) Chia, W. J.; Chung, Y. W. *J. Vacuum Sci. Technol. A* **1995**, *13*, 1687.
(8) Chia, W. J.; Chung, Y. W. *Intermetallics* **1995**, *3*, 505.
(9) Aoki, K.; Izumi, O. *Nippon Kinzoku Gakkaishi* **1979**, *43*, 1190.
(10) Liu, C. T.; White, C. L.; Horton, J. A. *Acta Metall.* **1985**, *33*, 213.
(11) Takasugi, T.; Masahashi, N.; Izumi, O. *Scripta Metall.* **1986**, *20*, 1317.
(12) Huang, S. C.; Briant, C. L.; Chang, K. M.; Taub, A. I.; Hall, E. L. *J. Mater. Res.* **1986**, *1*, 60.
(13) Masahashi, N.; Takasugi, T.; Izumi, O. *Acta Metall.* **1988**, *36*, 1823.
(14) White, C. L.; Padgett, R. A.; Liu, C. T.; Yalisove, S. M. *Scripta Metall.* **1984**, *18*, 1417.
(15) Liu, C. T.; White, C. L. *Acta Metall.* **1987**, *35*, 643.
(16) Briant, C. L.; Taub, A. I. *Acta Metall.* **1988**, *36*, 2761.
(17) Schulson, E. M.; Weihs, T. P.; Viens, D. V.; Baker, I. *Acta Metall.* **1985**, *33*, 1587.
(18) Schulson, E. M.; Weihs, T. P.; Baker, I.; Frost, H. J. *Acta Metall.* **1986**, *34*, 1395.
(19) Khadkikar, P. S.; Vedula, K.; Shable, B. S. *Metall. Trans. A* **1987**, *18*, 425.
(20) King, A. H.; Yoo, N. H. *Scripta Metall.* **1987**, *21*, 1115.
(21) Gleason, N. R.; Gerken, C. A.; Strongin, D. R. *Appl. Surf. Sci.* **1993**, *72*, 215.
(22) Ochiai, S.; Oya, Y.; Suzuki, T. *Acta Metall. Mater.* **1984**, *32*, 289.
(23) Guard, R. W.; Westbrook, J. H. *Trans. TMS-AIME* **1959**, *215*, 807.
(24) Staton-Bevan, A. E.; Rawlings, R. D. *Phys. Status Solidi A* **1975**, *29*, 613.
(25) Takasugi, T. *Acta Metall. Mater.* **1991**, *39*, 2157.
(26) George, E. P.; Liu, C. T.; Pope, D. P. *Scripta Metall. Mater.* **1993**, *28*, 857.
(27) Stulen, R. H.; Thiel, P. A. *Surf. Sci.* **1985**, *157*, 99.
(28) Barteau, M. A.; Madix, R. J. *Surf. Sci.* **1984**, *140*, 108.
(29) Au, C.-T.; Breza, J.; Roberts, M. W. *Chem. Phys. Lett.* **1979**, *66*, 340.
(30) Carley, A. F.; Rassias, S.; Roberts, M. W. *Surf. Sci.* **1983**, *135*, 35.
(31) Pirug, G.; Knauff, O.; Bonzel, H. P. *Surf. Sci.* **1994**, *321*, 58.
(32) Fuggle, J. C.; Watson, L. M.; Fabian, D. J. *Surf. Sci.* **1975**, *49*, 61.
(33) Kim, K. S.; Winograd, N. *Surf. Sci.* **1974**, *43*, 625.
(34) Haber, J.; Stoch, J.; Ungier, L. *J. Electron. Spectrosc. Relat. Phenom.* **1976**, *9*, 459.
(35) Joyner, R. W.; Roberts, M. W. *Chem. Phys. Lett.* **1974**, *28*, 246.
(36) Kiss, J.; Solymosi, F. *Surf. Sci.* **1986**, *177*, 191.
(37) Lide, D. R. *CRC Handbook of Chemistry and Physics*, 79th ed.; CRC Press: Boca Raton, FL, 1998; Chapter 9.
(38) Wang, Y.; Fan, J.; Trenary, M. *Chem. Mater.* **1993**, *5*, 192.